A. Colliander, J. Lahtinen, S. Tauriainen, J. Pihlflyckt, J. Lemmetyinen, M. T. Hallikainen, Sensitivity of Airborne 36.5-GHz Polarimetric Radiometer's Wind-Speed Measurement to Incidence Angle, IEEE Transactions on Geoscience and Remote Sensing, vol. 45, no. 7, pp. 2122-2129, July 2007.

Sensitivity of Airborne 36.5-GHz Polarimetric Radiometer's Wind-Speed Measurement to Incidence Angle

Andreas Colliander, *Associate Member, IEEE*, Janne Lahtinen, *Member, IEEE*, Simo Tauriainen, Jörgen Pihlflyckt, Juha Lemmetyinen, and Martti T. Hallikainen, *Fellow, IEEE*

***Abstract*—The Helsinki University of Technology's airborne fully polarimetric profiling radiometer at 36.5 GHz has been used for wind-vector measurements over the Gulf of Finland. The results, collected in a series of measurements over a period of two years, are presented in this paper. The Fourier coefficients of the harmonics of the first three modified Stokes parameters (in brightness temperature) have been solved, and their behavior as a function of the measurement incidence angle and the wind speed has been examined, resulting in a linear model in the measurement range. In this paper, we show a clear relationship between the incidence angle and the third modified Stokes parameter (in brightness temperature), which has been used to compensate for aircraft motion during measurements. Furthermore, the sensitivity of the wind-speed measurement to the incidence angle has been studied, and a model for wind-speed retrieval as a function of the harmonic coefficients and incidence angle was developed.**

***Index Terms*—Polarimetric radiometer, Stokes parameters, wind speed.**

I. Introduction

THE MARITIME wind-vector retrieval using a polarimetric radiometer has been one of the key points of interest in passive microwave remote sensing as of the early 1990s. The sensitivity of sea-surface brightness temperatures to ocean wind speed and direction has been demonstrated in many studies (e.g., [1]–[8]). Furthermore, the launch of the WindSat satellite in January 2003 [9] has opened the possibilities for global applications (e.g., [10]–[12]).

The results presented in this paper were obtained with the airborne fully polarimetric radiometer (FPoR) developed in the Laboratory of Space Technology, Helsinki University of Technology (TKK) [13]; the radiometer measures the so-called modified Stokes parameters in brightness temperature, which are defined under the Rayleigh–Jeans approximation as [14]

$$\mathbf{T} = \begin{bmatrix} T_v \\ T_h \\ T_3 \\ T_4 \end{bmatrix} = \frac{\lambda^2}{k_B \eta B} \begin{bmatrix} \langle |E_v|^2 \rangle \\ \langle |E_h|^2 \rangle \\ 2\mathrm{Re}\langle E_v E_h^* \rangle \\ 2\mathrm{Im}\langle E_v E_h^* \rangle \end{bmatrix} \tag{1}$$

where T_v, T_h, T_3, and T_4 are the brightness temperatures of the vertically and horizontally polarized radiation and the third and fourth Stokes parameter, respectively, λ is the wavelength, k_B is the Boltzmann's constant, η is the impedance of the medium, B is the bandwidth, and E_v and E_h are the vertically and horizontally polarized electric fields. The brackets stand for infinite time average. For simplicity, the term the Stokes parameters is applied in the following for the modified Stokes parameters in brightness temperature.

To describe the behavior of the Stokes parameters as a function of wind direction, an established method (e.g., [15] and [16]) is to use a second-order harmonic model

$$T_v \cong T_{v0} + T_{v1}\cos\phi + T_{v2}\cos 2\phi \tag{2}$$

$$T_h \cong T_{h0} + T_{h1}\cos\phi + T_{h2}\cos 2\phi \tag{3}$$

$$T_3 \cong T_{31}\sin\phi + T_{32}\sin 2\phi \tag{4}$$

$$T_4 \cong T_{41}\sin\phi + T_{42}\sin 2\phi \tag{5}$$

where ϕ is the wind direction. The first harmonics account for the upwind/downwind asymmetry of the surface, and the second harmonics account for the upwind/crosswind asymmetry of the surface. The Fourier coefficients of the two harmonic components, as well as the zeroth-order terms (offsets) of the first and second Stokes parameters, are functions of several parameters. We have assumed, here, that the harmonic coefficients are only dependent on surface wind speed, incidence angle, and frequency.

The dependence of a harmonic coefficient on wind speed and incidence angle is examined in this paper. Earlier studies (see Table I) have considered the dependence of the Stokes parameters on incidence angle, but the incidence angle variations of the third Stokes parameter have not been studied in detail previously.

In this paper, the dependence between the incidence angle and the first three Stokes parameters is presented over the measurement range. Using the obtained results, the incidence

Manuscript received May 31, 2006; revised November 21, 2006. This work was supported in part by Ulla Tuominen, by Jenny and Antti Wihuri, by Walter Ahlström, and by the Finnish Cultural Foundations.

A. Colliander was with the Laboratory of Space Technology, Helsinki University of Technology (TKK), 02150 Espoo, Finland. He is now with the European Research and Technology Centre, European Space Agency, 2200 AG Noordwijk, the Netherlands (e-mail: andreas.colliander@esa.int).

J. Lahtinen is an independent consultant (e-mail: spaceman@elisanet.fi).

S. Tauriainen, J. Lemmetyinen, and M. T. Hallikainen are with the Helsinki University of Technology (TKK), 02150 Espoo, Finland (e-mail: simo.tauriainen@tkk.fi; jlemmety@cc.hut.fi; martti.hallikainen@tkk.fi).

J. Pihlflyckt was with the Helsinki University of Technology (TKK), 02150 Espoo, Finland. He is now with Ajeco Ltd., 02210 Espoo, Finland (e-mail: jorgen.pihlflyckt@tkk.fi).

Digital Object Identifier 10.1109/TGRS.2007.894936

TABLE I
REPORTED POLARIMETRIC MEASUREMENTS OF MARITIME WINDS

Params[1]	$f\,[GHz]$	θ[2]	**Location**	**Year**	**Ref.**
$T_{v,h,3}$	10.7	53°	Labrador Sea	97	[7]
$T_{v,h,3,4}$	10.7	50°	Global	03-	[9][3]
T_3, Q	20	0°	Pacific O.[4]	91	[1]
$T_{v,h,3}, Q$	19.35	30,40,50°	NDBC[5]	93	[2]
$T_{v,h,3,4}, Q$	19.35	45,55,65°	NDBC[5]	94-96	[3],[4]
T_3, Q	16.26	45°	Danish Coast	96	[5]
$T_{3,4}, Q$	16	55°	North Sea	98	[8]
$T_{v,h,3,4}$	18.7	55°	Global	03-	[9][3]
T_3, Q	37	0°	Pacific O.[4]	91	[1]
T_3, Q	37	0°	Atlantic O.	92	[6]
$T_{v,h,3}, Q$	37	45,55,65°	NDBC[5]	94-96	[3],[4]
$T_{v,h,3}$	37	53°	Labrador Sea	97	[7]
$T_{3,4}, Q$	34	50°	North Sea	98	[8]
$T_{v,h,3,4}$	37	53°	Global	03-	[9][3]
$T_{v,h,3,4}$	36.5	43-58°	Baltic Sea	02-04	This,[13]

1) As defined in Equation (1), and $Q = T_v - T_h$.

2) Incidence angle (off nadir).

3) Several publications, for example [10]-[12].

4) North Western Pacific Ocean.

5) National Data Buoy Center, Californian Coast.

angle dependence of the third Stokes parameter was also accounted for in data postprocessing. Furthermore, the sensitivity of the coefficients of these Stokes parameters to the wind speed is estimated as a function of the incidence angle. Also, a model for wind-speed retrieval as a function of the harmonics and incidence angle was developed.

In [17], we introduced a model for the sensitivity of wind-speed measurement to the incidence angle and presented a model on the third Stokes parameter's dependence on incidence angle; this paper gives a detailed description of these models, applied data analysis, and developed wind-speed-retrieval model. In comparison to the study in [17], the data were reprocessed using several improvements in the processing algorithm, and the results are compared with the improved model by Yueh *et al.* [12].

II. TKK AIRBORNE FPOR

A. Instrument Description

TKK's airborne FPoR was used for this paper. The radiometer operates at 36.5 GHz, and it uses direct cross-correlation technique with analog correlators for solving all four Stokes parameters simultaneously. It has a radiometric resolution of about 0.2 K for the orthogonal polarizations and 0.3 K for the third and fourth Stokes parameters with an integration time of 1 s. The absolute accuracy is estimated to be 0.5 K (a detailed description of the radiometer can be found in [13]).

The FPoR is integrated into the profiling subsystem of the HUTRAD radiometer system, which consists of several major assemblies including six other radiometers at 1.4–94-GHz range [18], [19].

TABLE II
FLIGHT DATES, WIND SPEEDS, SURFACE TEMPERATURES, AND CLOUD CONDITIONS

Flight No.	**Date**	**WS** $[m/s]$	T_S $[^\circ C]$	**Clouds**
1	27 Mar 2002	6.7	+1.9	clear
2	28 Mar 2002	8.6	+1.9	clear
3	5 Dec 2003	12.0	+3.1	cloudy
4	7 Apr 2004	8.1	+1.2	clear
5	22 Apr 2004	10.9	+1.0	partial

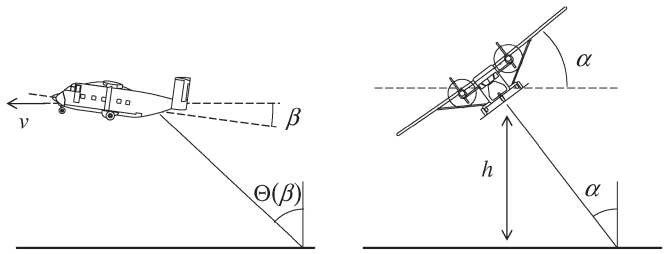

Fig. 1. Measurement geometry. The incidence angle was varied by changing the roll α and pitch β angle of the aircraft during the circular flights: α was varied about 40° and β about 4° (nominal value of Θ being 43°). The ground speed v was about 55 m/s (varying between 50–60 m/s), and the flight height h was about 1000 m.

B. Calibration

The calibration of the FPoR is presented in detail in [20]. In general terms, a fully polarimetric calibration target is applied to generate linearly independent sets of precisely known Stokes parameters. The target consists of cold and hot absorber loads, a polarizer grid, a retardation plate, and a pedestal with a rotary mechanism. The cold load is implemented using an absorber cooled down with liquid nitrogen.

III. MEASUREMENT FLIGHTS

Data were collected in five measurement flights during 2002–2004. The flight dates are presented in Table II. Each experiment consisted of a set of circles flown over the Kalbå dagrund area on the Gulf of Finland, the Baltic Sea. Between each set of circles, the incidence angle of the antenna beam was altered by changing the roll and pitch angles of the aircraft; the obtained incidence angles ranged from 43° to 58°. Altogether, 29 datasets were collected during five experimental flights; each dataset contains data with a relatively constant incidence angle and wind speed.

Fig. 1 illustrates the measurement geometry. The antenna footprint on the surface ranged from about 100 × 130 m to about 130 × 250 m. The attitude and speed of the aircraft were measured using two redundant systems: an attitude GPS navigation system and an inertial navigation system.

The ground-truth data were collected by the Kalbå dagrund weather station, which is an open-sea station in the measurement area. The collected ground-truth parameters include wind speed, wind direction, air temperature, and air pressure. The wind speed in the experiments ranged from 6.7 to 12.0 m/s. The measured wind-speed values (scaled to 10-m height above sea level [21]) during the experiments are depicted in Table II. The

weather station measured wind speed and direction only once in an hour, which generated some uncertainty. Therefore, the measured T_3 data were used to determine the wind direction for individual datasets. It is noted that, when coincided in time, the measured wind direction was always within few degrees with that determined using T_3 data. The only exception was flight number 1; due to low wind speed, the T_3 signal was weak and determination of wind direction inaccurate. For flight number 1, *in situ* measurement data were used for wind direction.

The physical temperature of the sea water and sea-surface salinity were estimated from measurements performed by the Finnish Institute of Marine Research.

IV. Theoretical Approach

A. Atmospheric Effects

The principles to retrieve the target brightness temperature, i.e., the brightness temperature of sea surface, are described in the following. The attitude data of the aircraft were applied to compensate for the mixing of the measured first three Stokes parameters due to aircraft roll (banking). The fourth Stokes parameter was not compensated for, since it is the measure of the circularly polarized radiation and, thus, independent of the linear polarization basis.

When correcting for the atmospheric effects, a radiative-transfer model was applied for the orthogonal polarizations. The model includes the following components: upwelling atmospheric brightness temperature (T_{UP}); atmospheric attenuation (τ); downwelling atmospheric brightness temperature (T_{DN}); and the reflection coefficient of the sea surface as a function of the relative wind direction and incidence angle $r(\phi, \theta)$. Scattering effects were assumed to be negligible, and they were ignored. Also, the following condition was assumed [22]:

$$\epsilon(\phi, \theta) = \frac{T_B(\phi, \theta)}{T_S} = 1 - r(\phi, \theta) \tag{6}$$

where $\epsilon(\phi, \theta)$ is the emission coefficient of the sea surface as a function of the relative wind direction and incidence angle, $T_B(\phi, \theta)$ is the brightness temperature of the sea surface as a function of the relative wind direction and incidence angle, and T_S is the physical temperature of the sea surface. Note that the atmospheric emission and attenuation are independent of the wind speed and relative wind direction. The applied radiative-transfer model, accounting for the azimuth dependence of the emissivity due to wind, can be written as

$$T_M(\phi, \theta) = T_{\mathrm{UP}} + \tau\epsilon(\phi, \theta)T_S + \tau T_{\mathrm{DN}}\left[1 - \epsilon(\phi, \theta)\right] \tag{7}$$

where $T_M(\phi, \theta)$ is the measured brightness temperature after compensating for the aircraft roll. Equations (6) and (7) yield

$$T_B(\phi, \theta) = \frac{T_M(\phi, \theta) - \tau T_{\mathrm{DN}} - T_{\mathrm{UP}}}{\tau(T_S - T_{\mathrm{DN}})} T_S. \tag{8}$$

In estimating the contribution of atmospheric radiation and attenuation, the principles presented in the study in [22] were followed. The pressure profile was estimated using the measured sea-level pressure and assuming exponential behavior. The kinetic-temperature profile was estimated using the measured surface air temperature and a statistical model. In retrieving the third and fourth Stokes parameter of the sea surface, only atmospheric attenuation was compensated for. This simplification is justified, because atmospheric emissions are essentially unpolarized. The Stokes parameters of the sea surface were retrieved with the above processing steps. Finally, the signal variations manifested by the incidence-angle fluctuations (due to aircraft motion) were compensated for T_v and T_h, using the emissivity model presented in the study in [23], and for T_3, using the model presented later in this paper (in Table V).

B. Wind-Speed Model and Sensitivity

The coefficients of the harmonics model in (2)–(5) were retrieved from the measured data sets. Note that, since no clear harmonic modulation was found, for the fourth Stokes parameter as a function of wind direction, the fourth Stokes parameter is not considered in this paper.

After solving the Fourier coefficients for each dataset, the coefficients were examined as a function of the incidence angle. A clear dependence for most of the coefficients can be found at each wind-speed value. This dependence shows very linear behavior within the measurement range (43°–58°); therefore, a linear model was fitted to these data.

Similarly, the harmonic coefficients show a linear behavior, as a function of wind speed in the 6.7–12.0-m/s range, when the incidence angle is kept constant. However, the slope of the coefficients with respect to the wind speed (i.e., the sensitivity of the harmonic coefficients on wind speed) is not constant as a function of the incidence angle. These sensitivities (slopes) can be plotted as a function of incidence angle. The sensitivity is defined here as the absolute value of the slope. Because the incidence angles were never exactly the same during the measurements at different wind speeds, the incidence angles applied for this analysis were interpolated/extrapolated equal using the linear model described earlier (between the Fourier coefficients and the incidence angle).

Furthermore, an empirical model, as a function of the harmonic coefficients and the incidence angle, for wind-speed retrieval is developed using the sensitivity (with the sign). For example, Yueh *et al.* [4] and Brown *et al.* [11] presented model functions for wind speed, and Yueh [24] introduced a theoretical model for incidence angle. Based on these models, and our results, it is reasonable to assume a linear behavior in the wind speed and incidence angle range of this paper. Although, semiempirical [11] and theoretical [24] models have also been presented previously, the choice of a purely empirical model (also used previously [7]) is justified by the fact that geophysical models of windy sea surface have remained uncertain [25]. The model is formulated as follows:

$$\mathrm{WS}(C, \theta) = (a_C\theta + b_C)C + c_C\theta + d_C \tag{9}$$

where WS is the value of wind speed, C is the harmonic coefficient, θ is the incidence angle, a_C and b_C are the slope

TABLE III
DATASETS OF THE HARMONIC COEFFICIENTS AND RESPECTIVE WIND SPEEDS AND INCIDENCE ANGLES

Data No.	WS $[m/s]$	θ [deg]	T_{v1} $[K]$	T_{v2} $[K]$	T_{h1} $[K]$	T_{h2} $[K]$	T_{31} $[K]$	T_{32} $[K]$
1	6.7	43.8	0.04	0.10	0.00	-0.11	-0.06	-0.19
2	6.7	46.4	0.12	0.02	0.07	-0.12	-0.01	-0.14
3	6.7	46.8	0.11	0.12	0.08	-0.01	-0.05	-0.16
4	6.7	47.6	0.05	0.13	0.05	-0.15	-0.03	-0.15
5	6.7	48.8	0.14	0.12	0.07	0.03	-0.07	-0.14
6	6.7	52.1	0.07	0.02	0.04	-0.04	-0.08	-0.02
7	6.7	52.2	-0.02	0.03	0.06	0.04	-0.09	-0.01
8	8.1	47.5	0.48	0.12	0.24	-0.71	-0.53	-0.66
9	8.1	51.4	0.63	-0.07	-0.12	-0.75	-0.68	-0.54
10	8.1	51.9	0.68	-0.02	0.33	-0.62	-0.72	-0.40
11	8.1	55.4	0.62	-0.23	0.15	-0.60	-0.61	-0.25
12	8.6	43.6	0.42	0.20	0.05	-0.73	-0.41	-0.71
13	8.6	46.0	0.49	0.16	0.13	-0.64	-0.40	-0.60
14	8.6	46.2	0.38	0.11	0.15	-0.52	-0.40	-0.52
15	8.6	47.3	0.40	0.10	0.18	-0.46	-0.41	-0.46
16	8.6	51.7	0.48	0.01	0.32	-0.67	-0.49	-0.38
17	8.6	51.8	0.54	-0.09	0.44	-0.62	-0.47	-0.38
18	8.6	52.3	0.45	-0.04	0.37	-0.41	-0.54	-0.20
19	10.9	45.4	0.78	0.26	0.02	-1.18	-0.86	-1.09
20	10.9	48.5	0.58	0.10	-0.28	-1.08	-0.86	-0.88
21	10.9	52.0	0.90	-0.05	0.55	-0.89	-0.82	-0.74
22	10.9	52.3	0.66	-0.03	0.24	-0.73	-0.75	-0.54
23	10.9	57.8	0.76	-0.35	0.21	-0.68	-0.59	-0.21
24	12.0	45.0	1.12	-0.11	0.02	-2.12	-1.26	-1.51
25	12.0	45.7	0.75	0.47	-0.48	-0.85	-1.07	-1.12
26	12.0	47.2	0.58	0.28	-1.04	-0.99	-1.24	-1.30
27	12.0	50.6	1.36	-0.07	0.17	-1.13	-1.05	-1.08
28	12.0	51.0	1.54	0.46	0.45	-0.26	-1.12	-0.93
29	12.0	54.9	0.85	-0.06	-0.75	-0.95	-1.14	-0.70

and offset of the sensitivity (with the sign) of the harmonic coefficient C, and c_C and d_C are the coefficients of the offset of the sensitivity (with the sign) of the harmonic C.

In previous studies [4], [7], [12], sophisticated nonlinear models have been presented for the dependence of the harmonics on the wind speed over a wide range of incidence angles and/or wind speeds. As stated in the previous paragraph, for the incidence angle and the wind-speed range analyzed in this paper, however, the linear model presents a simple and accurate way to describe the incidence angle dependence and, particularly, the sensitivity of the coefficients to the wind speed.

V. EXPERIMENTAL RESULTS

Table III shows all 29 obtained datasets of harmonic coefficients with wind-speed values and incidence angles. In general, the measured brightness temperatures show relatively little deviation from curves given by (2)–(4) with the coefficients of Table III. However, during measurements flights numbers 3 and 5, the sky was at least partially covered with clouds, which degraded the data a little bit by increasing the deviation of the data points from the fitted curve. This can be shown in Table IV,

TABLE IV
STANDARD DEVIATIONS OF THE MEASUREMENT DATA WITH RESPECT TO THE FITTED CURVE

Flight No.	**WS** $[m/s]$	**Clouds**	T_v $[K]$	T_h $[K]$	T_3 $[K]$
1	6.7	clear	0.170	0.227	0.192
2	8.6	clear	0.157	0.269	0.190
3	12.0	cloudy	0.712	1.424	0.346
4	8.1	clear	0.207	0.333	0.222
5	10.9	partial	0.225	0.419	0.310

TABLE V
SLOPES OF THE HARMONIC COEFFICIENTS VERSUS THE INCIDENCE ANGLE WITH THE WIND SPEED

WS $[m/s]$	T_{v1} $[K/^\circ]$	T_{v2} $[K/^\circ]$	T_{h1} $[K/^\circ]$	T_{h2} $[K/^\circ]$	T_{31} $[K/^\circ]$	T_{32} $[K/^\circ]$
6.7	-0.006	-0.009	0.002	0.015	-0.005	0.023
8.1	0.019	-0.043	-0.008	0.014	-0.011	0.053
8.6	0.009	-0.030	0.040	0.011	-0.014	0.045
10.9	0.005	-0.049	0.032	0.043	0.023	0.071
12.0	0.026	-0.017	0.004	0.078	0.008	0.067

where the averaged standard deviations (with respect to the fitted curve) of the measurements for each of the first three Stokes parameters are listed. Note that the standard deviation includes both instrumental and geophysical noise.

A. Dependency on Incidence Angle

Fig. 2 shows the harmonic Fourier coefficients of the first, second, and third Stokes parameter as a function of the incidence angle at three different wind-speed values (namely 6.7, 8.6, and 10.9 m/s). The linear fits are illustrated with lines. The data collected at the two other wind speeds (8.1 and 12.0 m/s) show similar behavior; they are left out in order to improve the clarity of the illustration. Also, the data collected from the third flight (wind speed at 12.0 m/s) suffered from the cloudy conditions, and particularly, the first and second Stokes parameters were affected (see Table IV). Table V lists the slopes (versus incidence angle) for all five experiments.

Yueh *et al.* presented in [4] a model for the harmonic coefficients as a function of the wind speed at three different incidence angles (45°, 55°, and 65°). This model was improved in the study in [12] using, for example, new WindSat satellite data. The coefficients of [12] are plotted in Fig. 2 at these incidence angles and respective wind speeds. For many harmonics, the resulted plots are similar to those obtained in this paper. In particular, T_{v2}, T_{h1}, and T_{32} show similar behavior. However, there are also differences, for example, in T_{v1}.

It can be seen that the harmonics of the third Stokes parameter have clear dependence on the incidence angle (Fig. 2, Table V). However, as shown in Table V, the sign of the dependence is different in flight numbers 3 and 5 (wind speeds at 12.0 and 10.9 m/s) from numbers 1, 2, and 4 (wind speeds at 6.7, 8.6, and 8.1 m/s), which show similar behavior as the model and measurements presented in the study in [24]. Note, however, that the flight numbers 3 and 5 were the ones contaminated

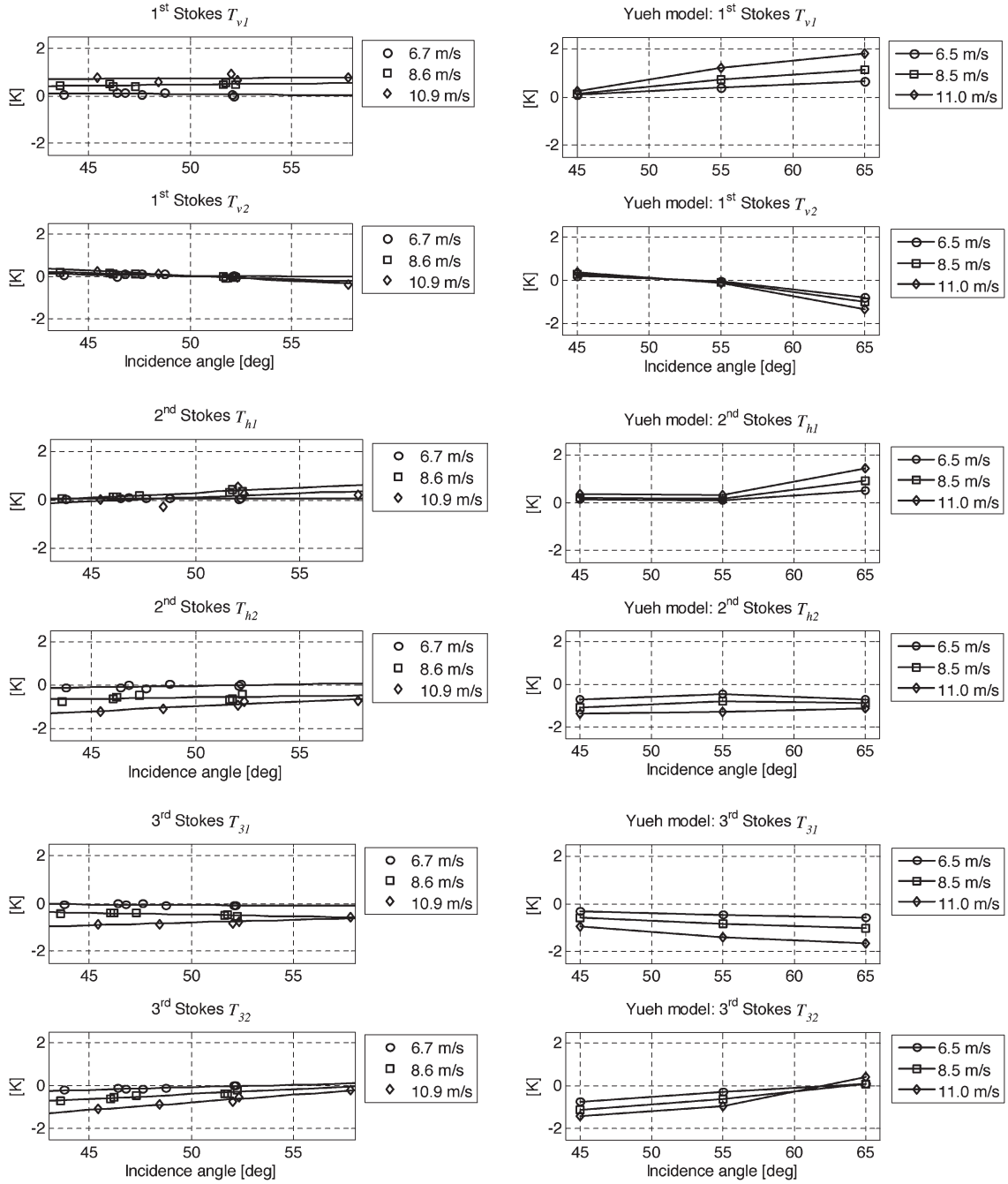

Fig. 2. Fourier coefficients of the first, second, and third Stokes parameter as a function of the incidence angle. (Left) Our experimental data. (Right) Values from the Yueh model [12]. In the plots of our experimental data, the lines show the linear fit to the dataset at each wind speed.

by the clouds, which could explain the unexpected behavior. On the other hand, T_3 is, in general, relatively undisturbed by clouds.

The potential sources for the harmonics' differences include differences of sea water's viscosity; in the measurements conducted for this paper, the water had a temperature of $+2$ °C on average and a salinity of approximately 5 psu. Both of these values are believed to be lower than the average conditions in the study in [12]. Also, different atmospheric conditions can cause some differences, as suggested in the study in [26]. Furthermore, the second-order processing differences between this paper and [12] may have caused some differences in the results; for example, we have taken advantage of mathematical methods and statistical estimates to assess atmospheric contribution, whereas [12] relied on radiometric-measurement data.

The obtained dependence slopes, presented in Table V, can be used for the correction of the incidence-angle deviations, for example, due to aircraft motion during measurement.

B. Sensitivity to Wind Speed

The obtained harmonics are dependent on the wind speed. As an example, the harmonic coefficients of the third Stokes

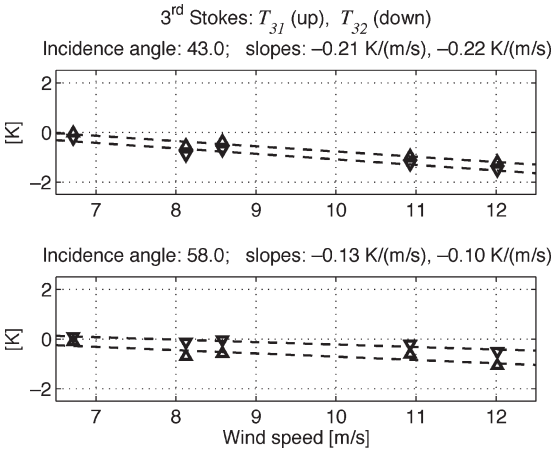

Fig. 3. Third Stokes parameter as a function of wind speed. The upper figure shows the first and second harmonic coefficient at an incidence angle of 43°, and the lower figure shows the first and the second harmonic coefficient at an incidence angle of 58°.

parameter are presented in Fig. 3 as a function of the wind speed. The linear fits are illustrated with dashed lines. The harmonics are shown for incidence angles of 43° and 58°. It can be clearly seen that the slopes are dependent on the incidence angles.

The absolute value of the slope with respect to the wind speed, or the sensitivity of the harmonic coefficients to the wind speed, is shown in Fig. 4 for the T_v, T_h, and T_3 parameters, respectively, as a function of incidence angle. It can be seen that the sensitivity of all coefficients has a clear dependence on the incidence angle. In most cases, the sensitivity increases with decreasing incidence angle, except in the case of T_{v1}. In the measurement range, the sensitivities of the harmonics on the wind speed have the following characteristic linear functions on incidence angle:

$$\Delta T_{v1}(\theta) = 0.0036\,\theta - 0.0221 \tag{10}$$

$$\Delta T_{v2}(\theta) = -0.0019\,\theta + 0.1095 \tag{11}$$

$$\Delta T_{h1}(\theta) = -0.0021\,\theta + 0.1634 \tag{12}$$

$$\Delta T_{h2}(\theta) = -0.0120\,\theta + 0.7611 \tag{13}$$

$$\Delta T_{31}(\theta) = -0.0052\,\theta + 0.4357 \tag{14}$$

$$\Delta T_{32}(\theta) = -0.0082\,\theta + 0.5732 \tag{15}$$

where $\theta = 43°$–$53°$.

C. Wind-Speed Model

The data set was used to develop a model for wind-speed retrieval based on (9). The harmonic coefficients of the third Stokes parameter are obviously best suited for this purpose due to their insensitivity to the clouds (see Table IV) and stronger dependence on the wind speed over the incidence angle range (particularly, the first harmonic coefficient). T_{v2} and T_{h1} are poorly suited for the use in the model due to the fact that they are very insensitive to the wind speed (see Fig. 2).

Table VI shows the coefficients of (9) for T_{v1}, T_{h2}, T_{31}, and T_{32}. T_{v2} and T_{h1} did not produce useful values due to the aforementioned reasons. Table VII shows the averaged result of the model applied to all data sets and root mean square (rms) of the deviation from the ground truth. The first harmonic coefficient of the third Stokes parameter produces the best result having most of the rms values under 1 m/s, which would indicate that this harmonic is the most accurate for wind-speed retrieval over the given incidence-angle range. This preliminary model can be used for the wind-speed retrieval (using measurements in

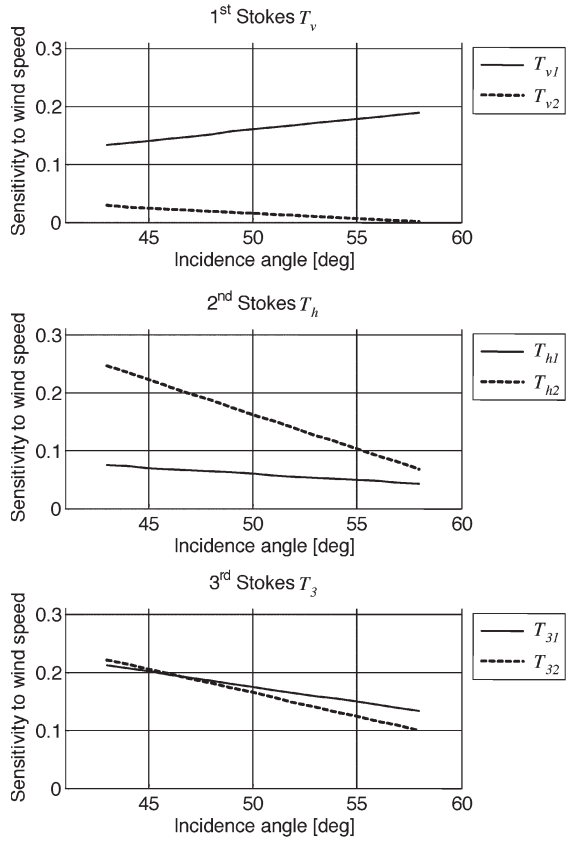

Fig. 4. Sensitivities (meters per second per Kelvin) of the first and second harmonic coefficients of the first three Stokes parameter to the wind speed as a function of the incidence angle.

TABLE VI
COEFFICIENTS FOR THE WIND-SPEED MODEL, (9)

Harmonic	a_C	b_C	c_C	d_C
T_{v1}	-0.153	14.076	0.025	4.382
T_{h2}	-0.931	36.054	-0.254	16.763
T_{31}	-0.187	3.296	-0.115	11.310
T_{32}	-0.401	12.745	0.167	-2.100

TABLE VII
RESULT OF THE WIND-SPEED MODEL, (9), USING THE VALUES OF TABLE VI FOR DIFFERENT HARMONIC COEFFICIENTS C

Ground	$C = T_{v1}$		$C = T_{h2}$		$C = T_{31}$		$C = T_{32}$	
[m/s]	mean	rms	mean	rms	mean	rms	mean	rms
6.7	6.1	0.7	4.9	2.1	6.1	0.7	6.7	0.3
8.1	9.4	1.3	11.6	3.6	9.4	1.3	10.0	1.9
8.6	8.6	0.3	9.6	1.5	8.3	0.3	8.9	0.6
10.9	10.2	1.0	13.7	2.9	10.2	1.0	11.4	1.0
12.0	12.4	2.2	13.6	4.2	12.3	0.6	13.5	1.7

multiple azimuth angles) up to this accuracy. The model for T_{31} reads ($\theta = 43^\circ - 58^\circ$)

$$\mathrm{WS}(T_{31}, \theta) = (-0.19\,\theta + 3.3)T_{31} - 0.12\,\theta + 11.31. \quad (16)$$

The model is to be expanded to a wider wind-speed and incidence-angle range as more measurement flights will be carried out. In the development process, the results given by this model can be compared to other models of other studies in order to find an optimum model.

VI. Conclusion

Five airborne-measurement campaigns have been conducted over the Gulf of Finland, the Baltic Sea. FPoR data have been collected at 36.5 GHz over an incidence-angle range of 43°–58° and for wind speeds between 6.7 and 12.0 m/s (scaled to 10-m height above sea level). In the measurement range, the results indicate a linear relationship between the harmonics of the first three Stokes parameters with the incidence angle. The coefficients for this relationship are presented; the coefficients of the third Stokes parameter were used to compensate for aircraft motion during measurements and, thus, to improve the quality of the data.

Furthermore, the sensitivities of the Fourier harmonics to wind speed have been investigated for T_v, T_h, and T_3 as a function of the incidence angle. In the measurement range, the sensitivities have clear linear dependence on the incidence angle. In general, the sensitivity decreases with increasing incidence angle, with the exception of the first harmonic of T_v. On the other hand, the swath width of an imaging polarimetric radiometer (airborne or spaceborne) decreases with decreasing incidence angle; the results presented here can be used to make tradeoff studies for an optimal incidence angle for each instrument and/or application. Finally, using the sensitivity, a preliminary empirical model function, as a function of the harmonic coefficients and the incidence angle, for wind-speed retrieval was developed promising an accuracy better than 1 m/s on average.

Acknowledgment

The authors would like to thank A. Pyy for the assistance in the experimental campaigns and also to the Finnish Institute of Marine Research and to the Finnish Meteorological Institute for their help for providing the ground-truth data.

References

[1] M. S. Dzura, V. S. Etkin, A. S. Khrupin, M. N. Pospelov, and M. D. Raev, "Radiometers–polarimeters: Principles of design and application for sea surface microwave emission polarimetry," in *Proc. IGARSS*, 1992, pp. 1432–1434.

[2] S. H. Yueh, W. J. Wilson, F. K. Li, S. V. Nghiem, and W. B. Ricketts, "Polarimetric measurements of sea surface brightness temperatures using an aircraft K-band radiometer," *IEEE Trans. Geosci. Remote Sens.*, vol. 33, no. 1, pp. 85–92, Jan. 1995.

[3] S. H. Yueh, W. J. Wilson, F. K. Li, S. V. Nghiem, and W. B. Ricketts, "Polarimetric brightness temperatures of sea surfaces measured with aircraft K- and Ka-band radiometers," *IEEE Trans. Geosci. Remote Sens.*, vol. 35, no. 5, pp. 1177–1187, Sep. 1997.

[4] S. H. Yueh, W. J. Wilson, S. J. Dinardo, and F. K. Li, "Polarimetric microwave brightness signatures of ocean wind directions," *IEEE Trans. Geosci. Remote Sens.*, vol. 37, no. 2, pp. 949–959, Mar. 1999.

[5] N. Skou and B. Laursen, "Measurement of ocean wind vector by an airborne, imaging polarimetric radiometer," *Radio Sci.*, vol. 33, no. 3, pp. 669–675, May/Jun. 1998.

[6] A. V. Kuzmin and M. N. Pospelov, "Measurements of sea surface temperature and wind vector by nadir airborne microwave instruments in joint United States/Russia internal waves remote sensing experiment JUSREX'92," *IEEE Trans. Geosci. Remote Sens.*, vol. 37, no. 4, pp. 1907–1915, Jul. 1999.

[7] J. R. Piepmeier and A. J. Gasiewski, "High-resolution passive polarimetric microwave mapping of ocean surface wind vector fields," *IEEE Trans. Geosci. Remote Sens.*, vol. 39, no. 3, pp. 606–622, Mar. 2001.

[8] B. Laursen and N. Skou, "Wind direction over ocean determined by an airborne, imaging, polarimetric radiometer system," *IEEE Trans. Geosci. Remote Sens.*, vol. 39, no. 7, pp. 1547–1555, Jul. 2001.

[9] P. W. Gaiser *et al.*, "The WindSat spaceborne polarimetric microwave radiometer: Sensor description and early orbit performance," *IEEE Trans. Geosci. Remote Sens.*, vol. 42, no. 11, pp. 2347–2361, Nov. 2004.

[10] M. H. Freilich and B. A. Vanhoff, "The accuracy of preliminary WindSat vector wind measurements: Comparison with NDBC buoys and QuickSCAT," *IEEE Trans. Geosci. Remote Sens.*, vol. 44, no. 3, pp. 622–637, Mar. 2006.

[11] S. T. Brown, C. S. Ruf, and D. R. Lyzenga, "An emissivity-based wind vector retrieval algorithm for the WindSat polarimetric radiometer," *IEEE Trans. Geosci. Remote Sens.*, vol. 44, no. 3, pp. 611–621, Mar. 2006.

[12] S. H. Yueh, W. J. Wilson, S. J. Dinardo, and S. V. Hsiao, "Polarimetric microwave wind radiometer model function and retrieval testing for WindSat," *IEEE Trans. Geosci. Remote Sens.*, vol. 44, no. 3, pp. 584–596, Mar. 2006.

[13] J. Lahtinen, J. Pihlflyckt, I. Mononen, S. Tauriainen, M. Kemppinen, and M. Hallikainen, "Fully polarimetric microwave radiometer for remote sensing," *IEEE Trans. Geosci. Remote Sens.*, vol. 41, no. 8, pp. 1869–1878, Aug. 2003.

[14] L. Tsang, J. A. Kong, and R. T. Shin, *Theory of Microwave Remote Sensing*. New York: Wiley, 1999.

[15] S. H. Yueh, R. Kwok, F. K. Li, S. V. Nghiem, and W. J. Wilson, "Polarimetric passive remote sensing of ocean wind vectors," *Radio Sci.*, vol. 29, no. 4, pp. 799–814, Jul./Aug. 1994.

[16] A. J. Gasiewski and D. B. Kunkee, "Polarized microwave emission from water waves," *Radio Sci.*, vol. 29, no. 6, pp. 1449–1466, Nov./Dec. 1994.

[17] A. Colliander, J. Lahtinen, S. Tauriainen, J. Pihlflyckt, J. Lemmetyinen, and M. Hallikainen, "Airborne ocean wind vector measurement using 36.5 GHz profiling polarimetric radiometer," in *Proc. IGARSS*, Seoul, Korea, 2005, pp. 4757–4760.

[18] M. Hallikainen, M. Kemppinen, J. Pihlflyckt, I. Mononen, T. Auer, K. Rautiainen, and J. Lahtinen, "HUTRAD: Airborne multifrequency microwave radiometer," in *Proc. ESA Workshop Millimetre Wave Technol. and Appl.: Antennas, Circuits and Syst.*, Espoo, Finland, 1998, pp. 115–120.

[19] K. Rautiainen, R. Butora, T. Auer, J. Kettunen, J. Kainulainen, I. Mononen, D. Beltrami, and M. T. Hallikainen, "Development of airborne aperture synthetic radiometer (HUT-2D)," in *Proc. IGARSS*, Jul. 2003, pp. 1232–1234.

[20] J. Lahtinen and M. Hallikainen, "HUT fully polarimetric calibration standard for microwave radiometry," *IEEE Trans. Geosci. Remote Sens.*, vol. 41, no. 3, pp. 603–611, Mar. 2003.

[21] S. D. Smith, "Coefficients for sea surface wind stress, heat flux, and wind profiles as a function of wind speed and temperature," *J. Geophys. Res.*, vol. 93, no. C12, pp. 15467–15472, Dec. 1988.

[22] F. Ulaby, R. Moore, and A. Fung, *Microwave Remote Sensing, Active and Passive*, vol. 1. Reading, MA: Addison-Wesley, 1981.

[23] P. Schluessel and H. Luthard, "Surface wind speeds over the North Sea from Special Sensor Microwave/Imager observations," *J. Geophys. Res.*, vol. 96, no. C3, pp. 4845–4853, Mar. 1991.

[24] S. H. Yueh, "Modeling of wind direction signals in polarimetric sea surface brightness temperatures," *IEEE Trans. Geosci. Remote Sens.*, vol. 35, no. 6, pp. 1400–1418, Nov. 1997.

[25] M. Zhang and J. T. Johnson, "Comparison of modeled and measured second azimuthal harmonics of ocean surface brightness temperature," *IEEE Trans. Geosci. Remote Sens.*, vol. 39, no. 2, pp. 448–452, Feb. 2001.

[26] M. N. Pospelov, "Surface wind speed retrieval using passive microwave polarimetry: The dependence on atmospheric stability," *IEEE Trans. Geosci. Remote Sens.*, vol. 34, no. 5, pp. 1166–1171, Sep. 1996.

Andreas Colliander (S'04–A'06) was born in Imatra, Finland, in 1976. He received the M.Sc. (tech.) and Lic.Sc. (tech.) degrees from the Helsinki University of Technology (TKK), Espoo, Finland, in 2002 and 2005, respectively, where he is currently working toward the D.Sc. (tech.) degree.

From 2001 to 2007, he was with the Laboratory of Space Technology, TKK, as a Research Scientist and a Project Manager. From 2003 to 2006, he was a Research Student at the National Graduate School for Remote Sensing, which was supported by the Finnish Ministry of Education and the Academy of Finland. He is currently with the European Space Research and Technology Centre, European Space Agency, Noordwijk, the Netherlands, as a Research Fellow. He is the author or coauthor of over 20 scientific publications on microwave remote sensing. His research is focused on microwave radiometry, with emphasis on polarimetric and interferometric radiometer systems and on the theoretical simulation of rough-surface backscattering.

Mr. Colliander was a recipient of the TKK Master's Thesis Award, an annual award for the top five master's theses of TKK.

Janne Lahtinen (S'98–M'03) received the M.Sc. (tech.), Lic.Sc. (tech.), and D.Sc. (tech.) degrees from the Helsinki University of Technology (TKK), Espoo, Finland, in 1996, 2001, and 2003, respectively.

From 1995 to 2002, he was with the Laboratory of Space Technology, TKK. From 1997 to 2002, he served as the Secretary of the Finnish National Committee of the Committee on Space Research, International Council for Science, and from 1999 to 2000, as the Secretary of the Space Science Committee, appointed by the Finnish Ministry of Education. From 2006 to 2007, he was an Advisor of the Finnish Space Committee. From 2002 to 2003, he was a Research Fellow at the European Research and Technology Centre, European Space Agency, Noordwijk, the Netherlands. From 2004 to 2006, he was with Elektrobit Microwave Ltd, Kauniainen, Finland, serving in various positions and, finally, as the Manager of Space and Security. From 2006 to 2007, he was the Director of Space at SF-Design Ltd. (Ylinen Electronics), Kauniainen, Finland. Since 2007, he has been an Independent Consultant. He is the author or coauthor of more than 40 publications in the area of microwave remote sensing and other fields. His research interests include microwave radiometer systems, calibration systems, and spacecraft hardware.

Dr. Lahtinen received the Third Place in the IEEE GRS-S Student Prize Paper Competition in 2000, the Young Scientist Award from the National Convention on Radio Science in 2001, and a Burgen Scholarship from Academia Europaea in 2004.

Simo Tauriainen was born in Oulu, Finland, in 1967. He received the M.Sc. (Tech.) and Lic.Sc. (Tech.) degrees from the Helsinki University of Technology (TKK), Espoo, Finland, in 1993 and 1998, respectively.

He is currently working in the Laboratory of Space Technology, TKK, responsible for measurement flight operations. His duties include measurement campaigns, aircraft-payload installations, aircraft-subsystem development, navigation systems, and microwave remote-sensing system development.

Jörgen Pihlflyckt is currently working toward the M.Sc. (Tech.) degree at the Helsinki Univeristy of Technology (TKK), Espoo, Finland.

From 1994 to 2007, he was with the Laboratory of Space Technology, TKK, where his responsibilities involved development of control systems for airborne radiometers. He is currently working as a Software Engineer at Ajeco Ltd., where his responsibilities mainly focus on web front ends for measurement and control systems. He has coauthored five articles on remote sensing.

Juha Lemmetyinen was born in Espoo, Finland, in 1977. He received the M.Sc. (Tech.) degree in electrical engineering from the Helsinki University of Technology (TKK), Espoo, Finland, in 2004.

He is currently working as a Research Scientist in the Laboratory of Space Technology, TKK. His research interests include microwave-radiometer development and calibration methods, and their applications for snow-cover monitoring.

Martti T. Hallikainen (F'93) received the Engineering Diploma (M.Sc.) and the Dr.Tech. degrees from the Helsinki University of Technology (TKK), Espoo, Finland, in 1971 and 1980, respectively.

In 1974–1975, he was the recipient of an Asla–Fulbright scholarship for graduate studies at the University of Texas, Austin. From 1981 to 1983, he was a Postdoctoral Fellow in the Remote Sensing Laboratory, University of Kansas. Since 1987, he has been a Professor of space technology at the Helsinki University of Technology, Espoo. In 1988, he established the Laboratory of Space Technology, TKK, and serves as its Director. In 1993–1994, he was a Visiting Scientist with the European Union's Joint Research Centre, Institute for Remote Sensing Applications, Italy. His research interests include development of microwave sensors for airborne and spaceborne remote sensing, development of methods to retrieve the characteristics of geophysical targets from satellite and airborne measurements, and cryospheric applications of remote sensing. His team recently completed the HUT-2D airborne interferometric L-band radiometer and is currently involved in technical development work and scientific projects concerning the near-future SMOS satellite.

Dr. Hallikainen was a member of the IEEE Geoscience and Remote Sensing (GRSS) Administrative Committee in 1988–2006 and served as President of the IEEE GRSS in 1996–1997. He was General Chair of the IGARSS'91 Symposium and Guest Editor of the Special IGARSS'91 Issue of the IEEE TRANSACTIONS ON GEOSCIENCE AND REMOTE SENSING (TGARS). He was Associate Editor of TGARS in 1992–2002. He served as Chair of the GRSS Nominations Committee in 1999–2006 and has been serving as GRSS Awards Committee Cochair since 2007. He has been Vice President of the International Union of Radio Science (URSI) since 2005 and served as the Chair of URSI Commission F in 2002–2005. He has been the national official member of URSI Commission F since 1988 and was Chair of the URSI Finnish National Committee in 1997–2005. He has been the Vice Chair of the Finnish National Committee of COSPAR since 2000. He was a member of the European Space Agency's (ESA) Earth Science Advisory Committee in 1998–2001. He has been a national delegate to the ESA Earth Observation Data Operations Scientific and Technical Advisory Group since 1995. He was Secretary General of the European Association of Remote Sensing Laboratories (EARSeL) in 1989–1993 and Chairman of the Organizing Committee for the EARSeL 1989 General Assembly and Symposium. He has been a member of the EARSeL Council since 1985. He was the recipient of three IEEE GRSS Awards: 1999 Distinguished Achievement Award; IGARSS'96 Interactive Paper Award; and 1994 Outstanding Service Award. He was the recipient of the IEEE Third Millennium Medal in 2000 and the Microwave Prize for the best paper in the 1992 European Microwave Conference.